NNMT promotes epigenetic remodeling in cancer by creating a metabolic methylation sink

Olesya A. Ulanovskaya, Andrea M. Zuhl, & Benjamin F. Cravatt

SUPPLEMENTARY RESULTS

Supplementary Figure Legends

Supplementary Dataset 1. Comparative metabolomic analysis of NNMT-OE versus GFP-OE renal carcinoma (769P), ovarian cancer (OVCAR3), and melanoma (MUM2C) cells. Tabs "769P-raw", "MUM2C-raw", and 'OVCAR3-raw" contain a complete list of all ions identified in untargeted metabolomic analysis and sorted by *P*-value. The following "769P-processed", "MUM2C-processed", and "OVCAR3-processed" tabs contain a list of deregulated metabolites ($P < 0.01$ and fold change between NNMT-OE and GFP-OE groups > 2), which were confirmed by manual extraction of MS1 chromatograms. Each tab contains values generated by XCMS analyte profiling software.

Supplementary Dataset 2. Gene expression analysis of NNMT-OE versus Y20A-OE renal carcinoma (769P) cells. Genes are sorted by fold change between NNMT-OE and Y20A-OE groups.

Supplementary Table 1. Targeted MRM measurements of cellular metabolites in various human cancer cell lines. Data are presented as means ± SEM in units of pmol/4 x 10^6 cells; methylation potential (MP) was calculates as [SAM]/[SAH]; N = 3-4/group; nd = not determined, na = not applicable.

Supplementary Table 2. Kinetic parameters of select methyltransferases. NNMT-sensitive and insensitive methylation events are controlled by methyltransferases with high and low K_m (K_i) values for SAM (SAH), respectively.

Supplementary Fig. 1. Cell migration assays with human lung and renal cancer cell lines. The aggressive cancer cell lines H226 (**a**, lung) and 768O (**b**, renal) exhibit much greater migratory activity compared to the less aggressive H522 (**a**, lung) and 769P (**b**, renal) cells. Data are presented as mean values ± SEM; N = 3 experiments/group; $^{**}P < 0.01$ for aggressive versus non-aggressive human cancer cell lines.

Supplementary Fig. 2. Generation of NNMT-OE models in melanoma and ovarian cancer cells. (**a**) Overexpression of NNMT containing FLAG-6-His epitope tag in non-aggressive MUM2C and OVCAR3 cells (NNMT-OE) confirmed by western blotting (upper panels) and substrate activity (bar graphs) assays. GFP-OE and Y20A-OE cells correspond to cancer cells infected with GFP-vector and a catalytically inactive NNMT mutant (Y20A), respectively. Western blotting revealed only exogenous NNMT levels as basal NNMT levels in both MUM2C and OVCAR3 cells were below detection limit. Western blot analysis confirmed overexpression of the NNMT-Y20A mutant, which did not show any significant activity as judged by NNMT activity assay. See **Supplementary Fig. 13** for full gel images. (**b**) NNMT-OE cells possess elevated levels of 1MNA compared to control cells. Data shown as mean values ± SEM; for metabolomics experiments N = 3-4/group; for substrate assay N = 2/group; $^{**}P < 0.01$ for NNMT-OE versus control (GFP-OE and Y20A-OE) groups.

Supplementary Fig. 3. NNMT contributes to aggressive properties of cancer cells. (**a**) NNMT-OE cells show enhanced migratory activity compared to GFP-OE and Y20A control cells in Transwell migration assays, in which serum starved cells were evaluated for their ability to migrate through 8 μm pore-sized membranes coated with 10 μg/ml collagen. Cells were allowed to migrate for 4 h. (**b**) si-NNMT SKOV3 cells show significantly decreased migration (4 h) and invasion (17 h) compared to si-Control cells. For both (**a**) and (**b**), assays were performed in RPMI1640 medium containing 10 μM methionine. (**c**) si-NNMT SKOV3 cells cultured in high methionine (100 μM) medium show no change in migration compared to si-Control cells. Data are presented as mean values ± SEM; N = 6 experiments/group. $^{*}P < 0.05$, $^{**}P < 0.01$ for NNMT-OE versus control (GFP-OE and Y20A-OE) groups or for si-NNMT versus si-control groups.

Supplementary Fig. 4. 1MNA does not affect cancer cell migration. GFP-OE 769P cells treated with 0.5 mM 1MNA for 48 h in low methionine (10 μM) medium show no change in migration rate (4 h) compared to untreated cells. Data are presented as mean values ± SEM; N = 3 experiments/group.

Supplementary Fig. 5. Metabolomic analysis shows elevated 1MNA and SAH levels in NNMT-OE cells relative to control cells. Extracted MS1 ion chromatograms and corresponding bar graphs (manual integration) showing elevated 1MNA and SAH levels in NNMT-OE MUM2C (**a**) and OVCAR3 (**b**) cells. Targeted LC-MS analysis with deuterated internal standards confirmed deregulation of SAH in NNMT overexpressing MUM2C (**c**) and OVCAR3 (**d**) cells. Data are presented as mean values ± SEM; N = 3-4 experiments/group; $^{**}P < 0.01$ for NNMT-OE versus control (GFP-OE and Y20A-OE) groups.

Supplementary Fig. 6. NNMT alters the methylation potential (MP) and epigenetic state of cancer cells grown in 20 and 10 μM methionine. (**a**, **b**) 20 μM methionine grown NNMT-OE 769P cells show reduced SAM and enhanced SAH levels (**a**) (and a correspondingly reduced MP) as well as reduced protein methylation (**b**) compared to control cells. (**c, d**) NNMT-OE 769P cells grown on 10 μM methionine show reductions in histone 3 and 4 methylation events compared to GFP-OE and Y20A-OE control lines as determined by Western blotting. Conversely, si-NNMT cells grown on 10 μM methionine show increases in most of these histone methylation events compared to si-Control cells. (**d**) Bar graphs quantifying representative methylation changes shown in (**c**) and **Fig. 4a**. For (**a**), data are presented as mean values ± SEM; N = 3 experiments/group. ** $P < 0.01$ for NNMT-OE versus GFP-OE groups; for (**d**), data are presented as mean values ± SEM; N = 3-6 experiments/group. $^{*}P < 0.05$ for NNMT-OE versus Y20A-OE groups. Western blot band intensity was first normalized to total histone 3 levels, followed by normalization of all samples to GFP-OE control group. See **Supplementary Fig. 14** for full gel images.

Supplementary Fig. 7. NNMT alters the methylation potential (MP) and epigenetic state of 769P cancer cells grown in 10 μM methionine. Similar changes in SAM and SAH levels were observed in NNMT-OE cells when analyzed by two different metabolite extraction protocols. (**a**) Metabolomes were prepared by adding extraction solution to cells harvested in ice-cold PBS. Shown are data taken from **Fig. 3c**, which are presented here for direct comparison to results from part **b**. (**b**) Metabolites were directly extracted from plated cells without any PBS washes (see **Online Methods** for detailed protocol).

Supplementary Fig. 8. NNMT overexpression or knockdown alters the methylation potential (MP) and epigenetic state of cancer cells grown in 10 μM methionine. (**a**) MUM2C cells cultured with 10 μM methionine show much lower cellular SAM levels compared to cells grown on 100 μM methionine (23 pmol/4 $\times 10^6$ cells in 10 μM methionine versus 415 pmol/4 $\times$ 10^6 cells in 100 μM methionine). NNMT-OE cells exhibit higher SAH levels (and a correspondingly lower MP) compared to GFP-OE and Y20A-OE when cells are grown in either 10 or 100 μM methionine (for 100 μM methionine data see **Supplementary Fig. 5**). (**b**) NNMT-OE MUM2C cells grown on low methionine show impaired histone methylation revealed by WB. No changes in histone methylation were observed when these cells were grown on high methionine medium. Bar graph shows representative methylation changes. (**c**) NNMT-OE MUM2C cells show decrease in PP2A methylation as determined by WB. (**d-f**) si-NNMT H226 cells show reduced NNMT expression (**d**), lower 1MNA levels (**d**), higher SAM levels (and a correspondingly higher MP) (**e**), and elevated histone methylation (**f**) compared to si-Control cells when cells are grown in 10 μM methionine. For (**a**), (**b**), (**c**), (**d**) and (**e**), data are presented as mean values ± SEM; for (**a**), (**d**) and (**e**), N = 3-4 experiments/group; for (**b, c**), N = 2-3 replicates/group. $^{*}P < 0.05$, $^{**}P < 0.01$ for NNMT-OE versus Y20A-OE group or for si-NNMT versus si-control groups. See **Supplementary Fig. 13** and **14** for full gel images.

Supplementary Fig. 9. Metabolic labeling experiment to study metabolism of 1MNA. 769P cells were treated with deuterated 1MNA (d_4-1MNA) and then profiled by LC-MS to reveal the formation of deuterated metabolites. 1MNA appears to be stable in cancer cells given that no deuterated metabolites except for d_4-1MNA were observed after 24 h. In contrast, when cells were treated with d_4-NA, several deuterated

metabolites, including d_4-NA, d_3-NA, d_4-1MNA, d_3-NMN, d_3-NAD^+ and d_3-NADH were observed. NADH levels were near the detection limit after 24 h, therefore NADH levels were measured after 4 h. Data are presented as mean values ± SEM; N = 3 experiments/group.

Supplementary Fig. 10. Protein methylation changes induced by NNMT are blunted by growing cells in high methionine. NNMT-OE cells did not show significant changes in histone methylation profiles (**a**) and protein arginine methylation (**b**) when grown in high (100 μM) methionine (Met) medium. Protein arginine methylation was profiled by using ASYM25 antibody, which recognizes asymmetrical dimethylated arginines. NNMT-OE, GFP-OE, and Y20A-OE cells grown in low (10 μM) methionine are shown for comparison. See **Supplementary Fig. 15** for full gel images.

Supplementary Fig. 11. 1MNA does not affect protein methylation profiles of cancer cells. Treatment of GFP-OE 769P cells with 0.5 mM 1MNA for 48 h produced a dramatic increase in cellular 1MNA (**a**), but did not affect histone and PP2A methylation (**b**). GFP-OE cells +/- 1MNA were compared to NNMT-OE cells as a positive control. All cells were grown in low (10 μM) methionine medium. See **Supplementary Fig. 15** for full gel images.

Supplementary Fig. 12. NNMT-OE regulates arginine methylation and doesn't affect global DNA methylation. (**a**, **b**) NNMT-OE cells show reduced levels of select protein arginine methylation events compared to GFP-OE and Y20A-OE control cells as determined by Western blotting using the ASYM25 antibody, which recognizes

asymmetrical dimethylated arginines. Methylation changes in NNMT-OE cells are marked with an asterisk. si-NNMT cells show a more limited number of changes in arginine methylation compared to si-Control cells. (**b**) Bar graphs quantifying the methylation change for the ~55 kDa protein highlighted by a red box in (**a**). (**c**) NNMT-OE 769P cells did not show significant differences in 5-methyl-2'-deoxycytidine content, when compared to GFP-OE and Y20A-OE cells. For all studies, cells were cultured in low (10 μM) methionine medium. For (**b**) and (**c**), data are presented as mean values ± SEM; N = 3-4 experiments/group. ** $P < 0.01$ for NNMT-OE versus control Y20A-OE groups.

Supplementary Fig. 13. Full gel images for **Figure 1a,c,d**, **Supplementary Figure 2a**, and **Supplementary Figure 8d**. Following protein transfer, nitrocellulose membranes were cut around 37 KDa and stained with anti-Tubulin (top, loading control) and anti-NNMT (bottom) antibodies.

Supplementary Fig. 14. Full gel images for **Figure 4a,c**, **Supplementary Figure 6b,c**, and **Supplementary Figure 8b,f**. Western blotting for (**a**) H3-total and H3K4 (me1, me2, me3); (**b**) H3K9 (me1, me2, me3) and PP2A (total, me, deme); (**c**) H3K27 (me2, me3), PP2A (total, me, deme), H3R17-ame2 and H4K20-me2. Following protein transfer, nitrocellulose membranes were cut and stained as shown. Unless otherwise noted, cells were grown on 10 μM methionine.

Supplementary Fig. 15. Full gel images for (**a**) **Supplementary Figure 10a** and (**b**) **Supplementary Figure 11b.** Following protein transfer, nitrocellulose membranes were cut and stained as shown.

Supplementary Dataset 1. See companion Excel file.

Supplementary Dataset 2. See companion Excel file

Supplementary Table 1.

Cell type	[Met][a]	Metabolite	GFP-OE	NNMT-OE	Y20A-OE	Fold change[b]	*P*-value[b]	Fold change[c]	*P*-value[c]
769P	100	1MNA	100.3 ± 6.2	1446 ± 96	78.8 ± 7.4	14	0.000	18	0.000
		SAH	25.1 ± 1.8	186 ± 16	26.6 ± 1.7	7.4	0.000	7.0	0.000
		SAM	240 ± 8	187 ± 12	211 ± 9	0.78	0.012	0.89	0.208
		Met	nd	nd	nd	nd	na	na	na
		MP (calc)	9.77 ± 0.91	1.02 ± 0.05	8.02 ± 0.75	0.10	0.000	0.13	0.000
769P	20	1MNA	41.1 ± 9.0	338 ± 35	nd	8.2	0.001	na	na
		SAH	25.5 ± 0.5	91.7 ± 11.6	nd	3.6	0.005	na	na
		SAM	36.9 ± 0.5	20.9 ± 2.6	nd	0.57	0.004	na	na
		Met	25.7 ± 0.7	21.9 ± 0.9	nd	0.85	0.029	na	na
		MP (calc)	1.45 ± 0.05	0.23 ± 0.01	nd	0.16	0.000	na	na
769P	10	1MNA	10.6 ± 0.9	61.5 ± 14	6.4 ± 1.5	5.8	0.004	9.6	0.008
		SAH	15.7 ± 1.7	29.2 ± 3.4	18.2 ± 1.6	1.9	0.007	1.6	0.028
		SAM	18.5 ± 1.1	6.7 ± 0.8	14.8 ± 1.0	0.36	0.000	0.45	0.001
		Met	18.8 ± 0.9	19.8 ± 0.9	25.1 ± 3.2	1.1	0.473	0.79	0.165
		MP (calc)	1.24 ± 0.18	0.23 ± 0.01	0.84 ± 0.13	0.19	0.001	0.27	0.004
MUM2C	10	1MNA	≤ 2[d]	167 ± 7	≤ 2[d]	≥ 84[d]	0.000	≥ 84[d]	0.000
		SAH	18.4 ± 1.7	37.8 ± 1.6	21.7 ± 1.0	2.0	0.002	1.7	0.000
		SAM	23.2 ± 0.1	18.8 ± 1.4	20.7 ± 1.6	0.81	0.124	0.91	0.461
		Met	19.2 ± 1.3	19.9 ± 2.3	26.5 ± 3.1	1.0	0.862	0.75	0.140
		MP (calc)	1.26 ± 0.11	0.5 ± 0.05	0.95 ± 0.04	0.40	0.002	0.52	0.000

Cell type	[Met]	Metabolite	si-Control	si-NNMT	Fold change	*p*-value
SKOV3	10	1MNA	134 ± 8.3	38.8 ± 1.9	0.29	0.000
		SAH	19.6 ± 1.1	12.2 ± 1.0	0.62	0.007
		SAM	4.6 ± 0.5	11.3 ± 1.3	2.5	0.007
		Met	44.1 ±2.2	37.4 ± 0.8	0.85	0.049
		MP (calc)	0.24 ± 0.04	0.92 ± 0.06	3.8	0.001
H226	10	1MNA	251 ± 7	76.6 ± 1.4	0.31	0.000
		SAH	25.9 ± 2.1	25.2 ± 1.6	1.0	0.811
		SAM	29.9 ± 2.5	46.2 ± 1.6	1.6	0.004

Met	32.8 ±3.4	41.2 ± 2.9	1.3	0.136
MP (calc)	1.16 ± 0.08	1.85 ± 0.14	1.6	0.006

[a] Methionine (Met) concentration in cell culture medium is shown in μM. For 100 μM methionine conditions, cells were grown in complete RPMI-1640 medium. For low methionine conditions, cells were grown for 48h on medium containing either 20 or 10 μM methionine.

[b] Fold changed calculated as NNMT-OE/GFP-OE; *P*-value for NNMT-OE and GFP-OE groups

[c] Fold changed calculated as NNMT-OE/Y20A-OE; *P*-value for NNMT-OE and Y20A-OE groups

[d] 1MNA signals were below the detection limit and are listed as ≤ 2 pmol/4 × 10^6 cells, leading to a minimal fold change of ≥ 84.

Supplementary Table 2.

Enzyme	K_m for SAM, (μM)	K_i for SAH, (μM)	Product	Sensitivity to NNMT
EZH1[a]	2.5	8.3	H3K27-me2/3	High
EZH2[a]	1.2	7.5	H3K27-me2/3	High
LCMT1[b]	1.3	3.0 (IC_{50})	PP2A-me	High
CARM1[a]	0.16	0.12	H3R17-me2a	Low
NNMT[c]	1.8	40-100 (IC_{50})	1MNA (IC_{50} = 50 μM)	

[a] Kinetic parameters have been previously reported by Richon et al[1].

[b] Kinetic parameters have been previously reported by Derua et al[2].

[c] Kinetic parameters have been previously reported[3,4,5].

References for Supplementary Table 2

1. Richon, V.M. *et al.* Chemogenetic Analysis of Human Protein Methyltransferases. *Chemical Biology & Drug Design* **78**, 199-210 (2011).
2. De Baere, I. *et al.* Purification of Porcine Brain Protein Phosphatase 2A Leucine Carboxyl Methyltransferase and Cloning of the Human Homologue†,‡. *Biochemistry* **38**, 16539-16547 (1999).
3. Rini, J., Szumlanski, C., Guerciolini, R. & Weinshilboum, R.M. Human liver nicotinamide N-methyltransferase: Ion-pairing radiochemical assay, biochemical properties and individual variation. *Clinica Chimica Acta* **186**, 359-374 (1990).
4. Aksoy, S., Szumlanski, C.L. & Weinshilboum, R.M. Human liver nicotinamide N-methyltransferase. cDNA cloning, expression, and biochemical characterization. *Journal of Biological Chemistry* **269**, 14835-14840 (1994).
5. Scheller, T., Orgacka, H., Szumlanski, C.L. & Weinshilboum, R.M. Mouse liver nicotinamide N-methyltransferase pharmacogenetics: biochemical properties and variation in activity among inbred strains. *Pharmacogenetics and Genomics* **6** (1996).

Supplementary Figure 1

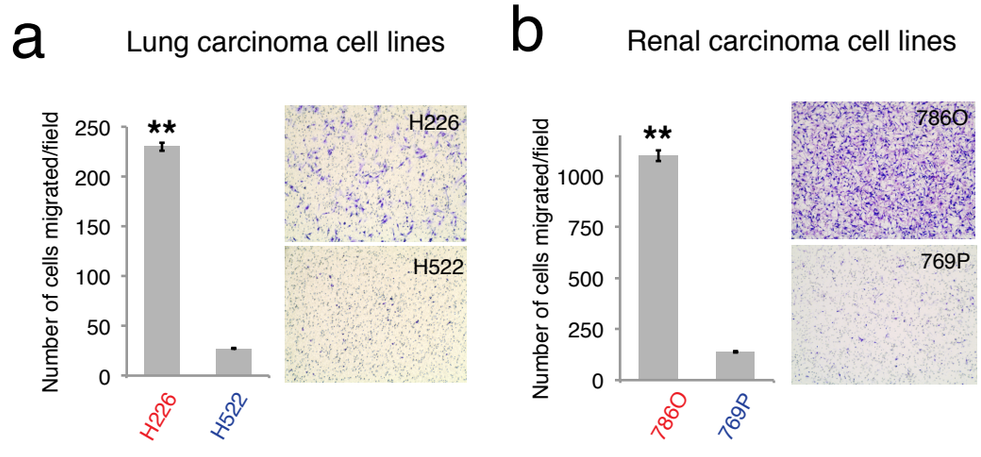

Supplementary Figure 2

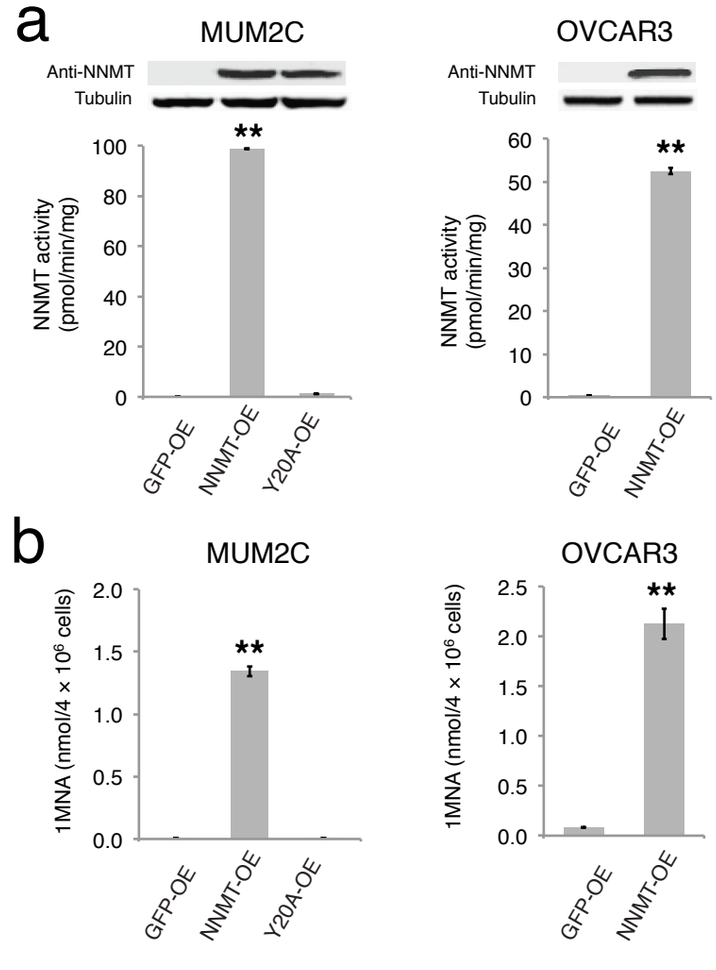

Supplementary Figure 3

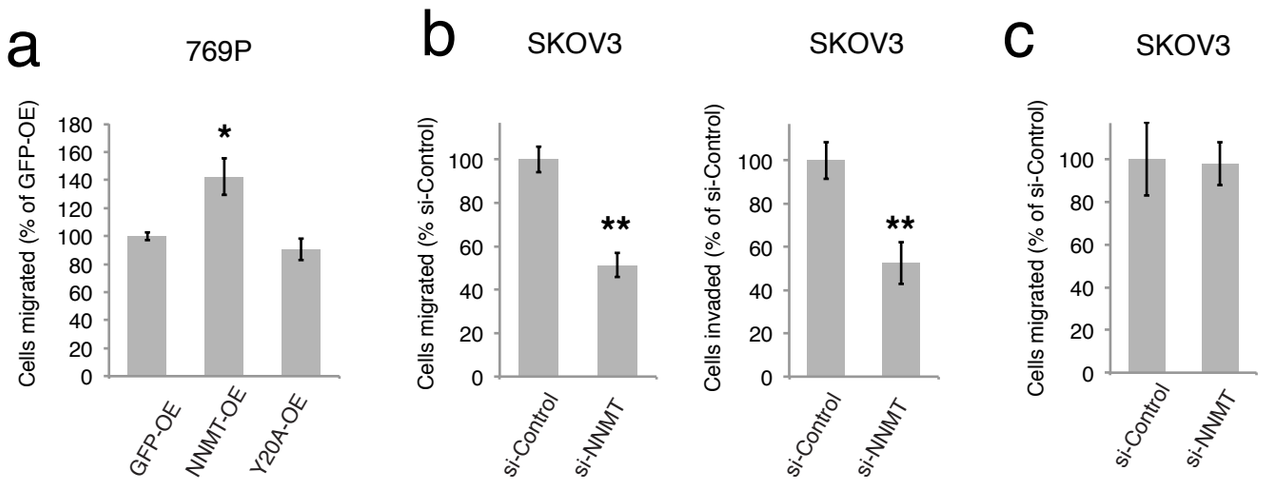

Supplementary Figure 4

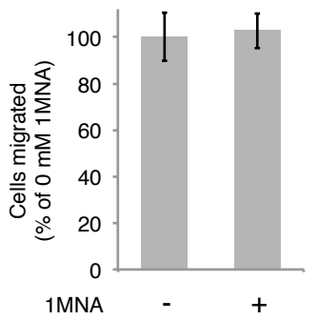

Supplementary Figure 5

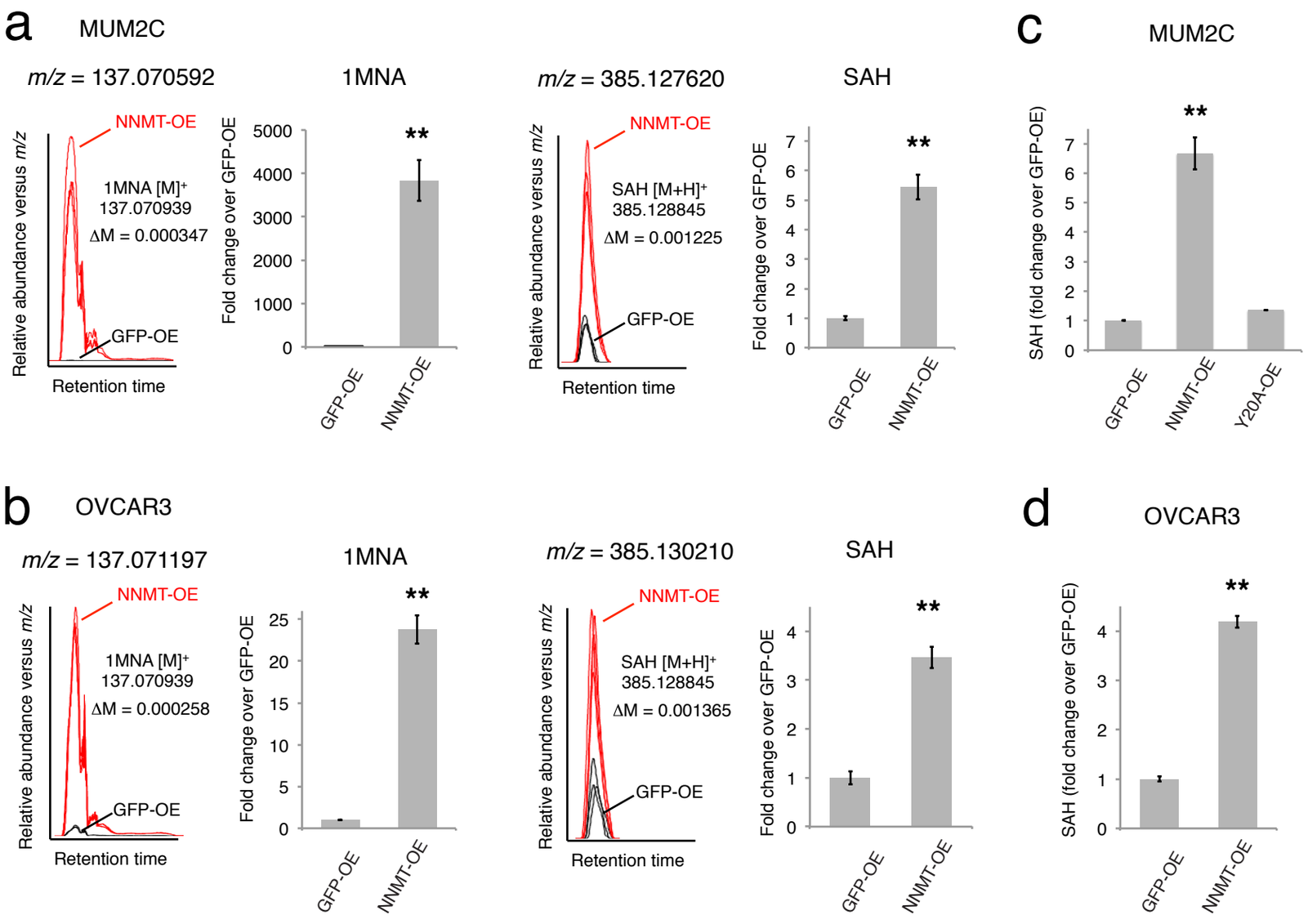

Supplementary Figure 6

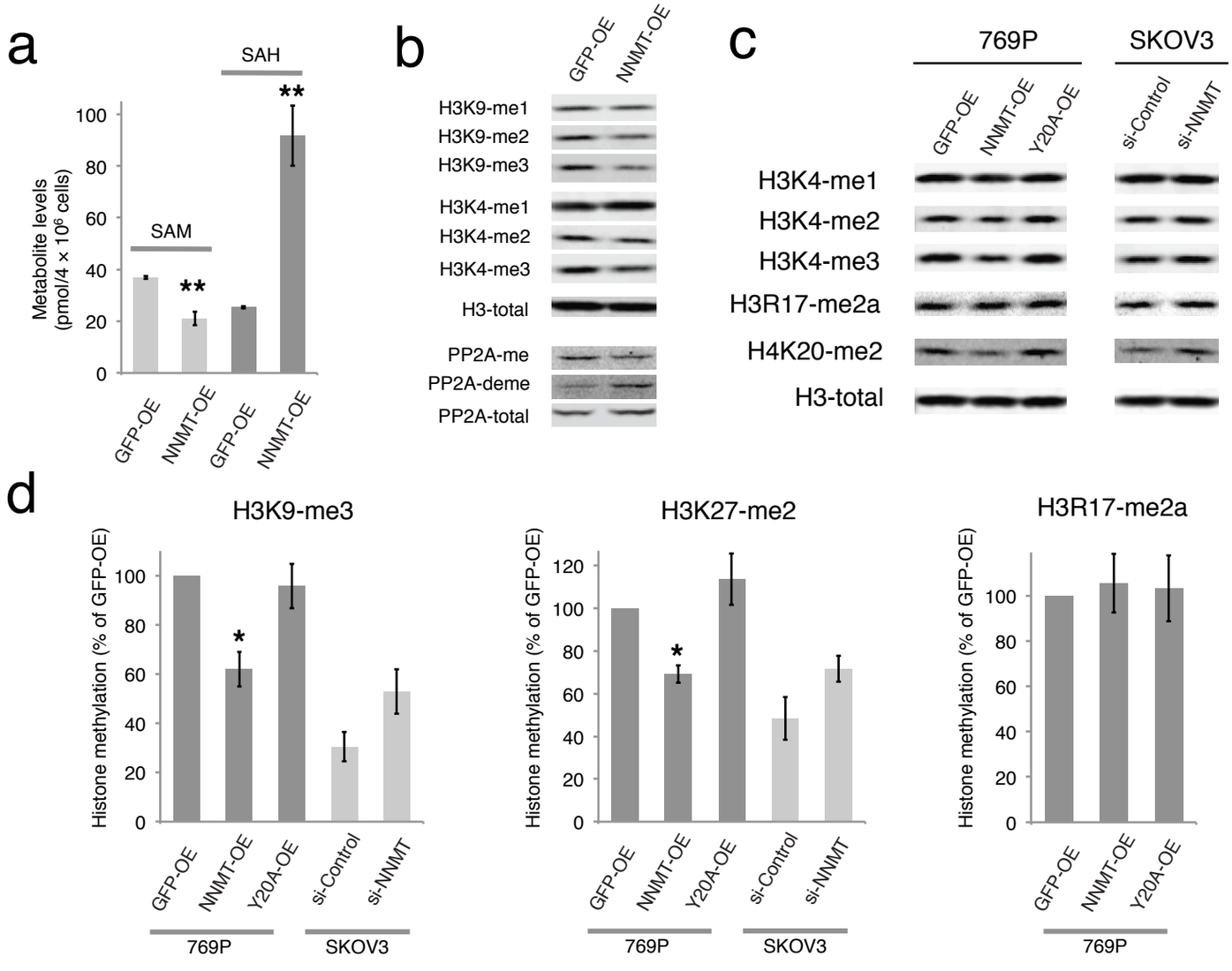

Supplementary Figure 7

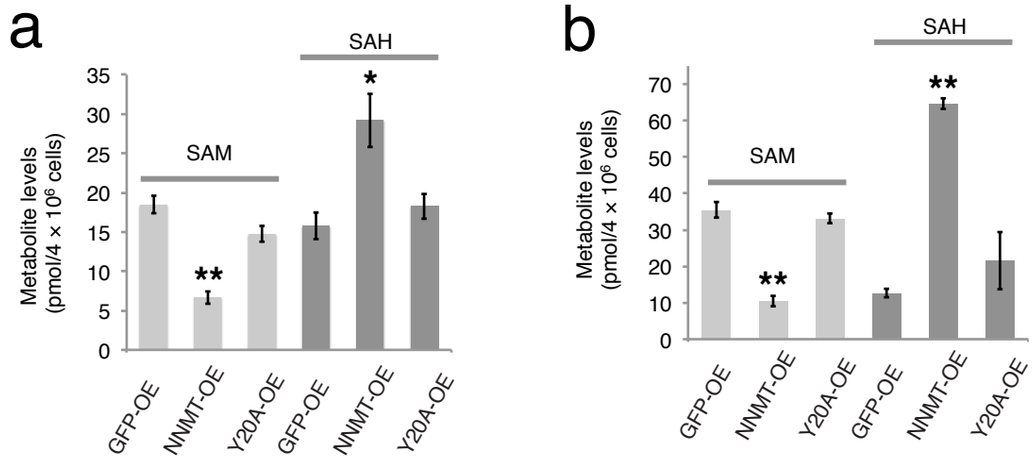

Supplementary Figure 8

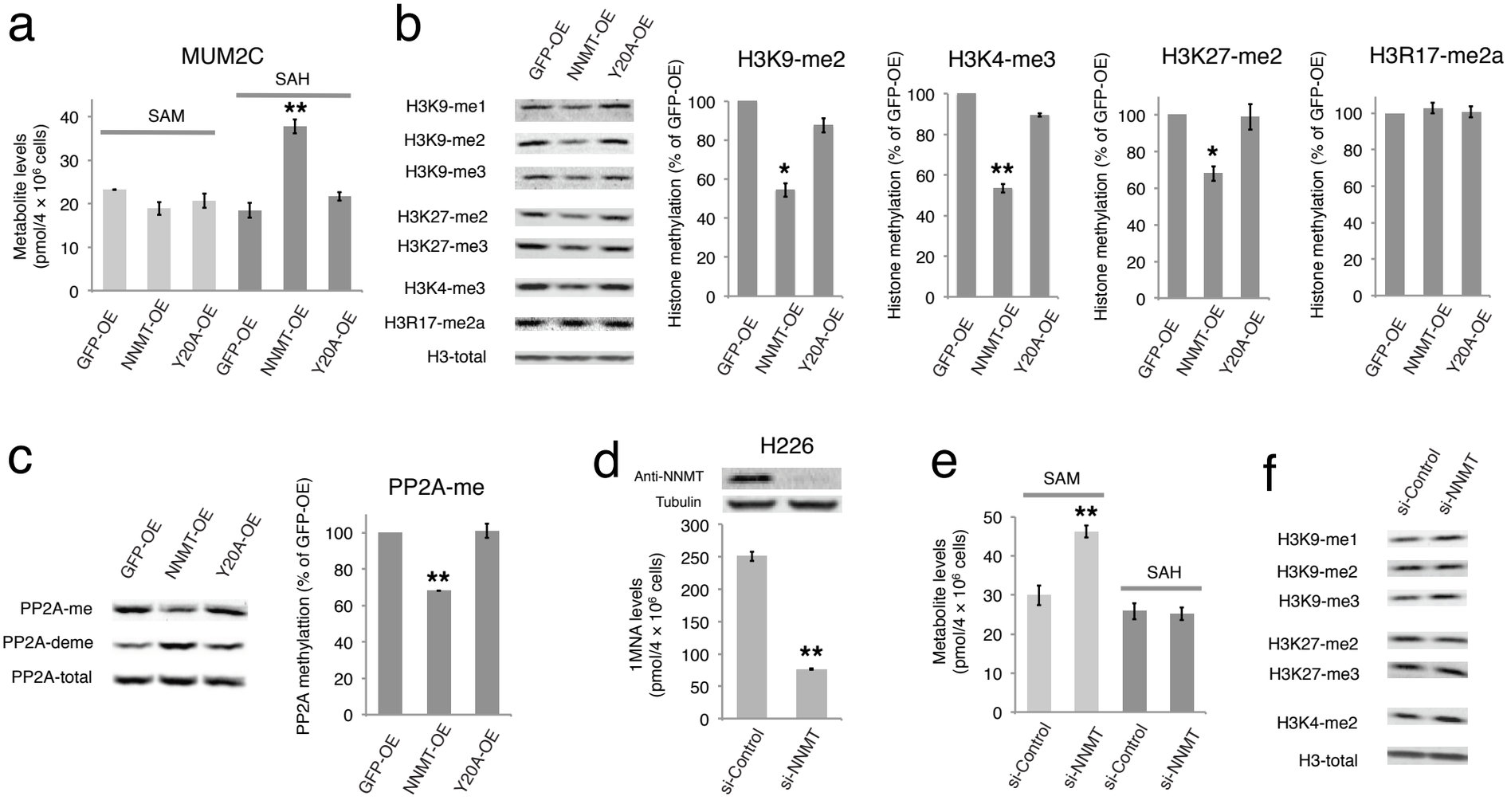

Supplementary Figure 9

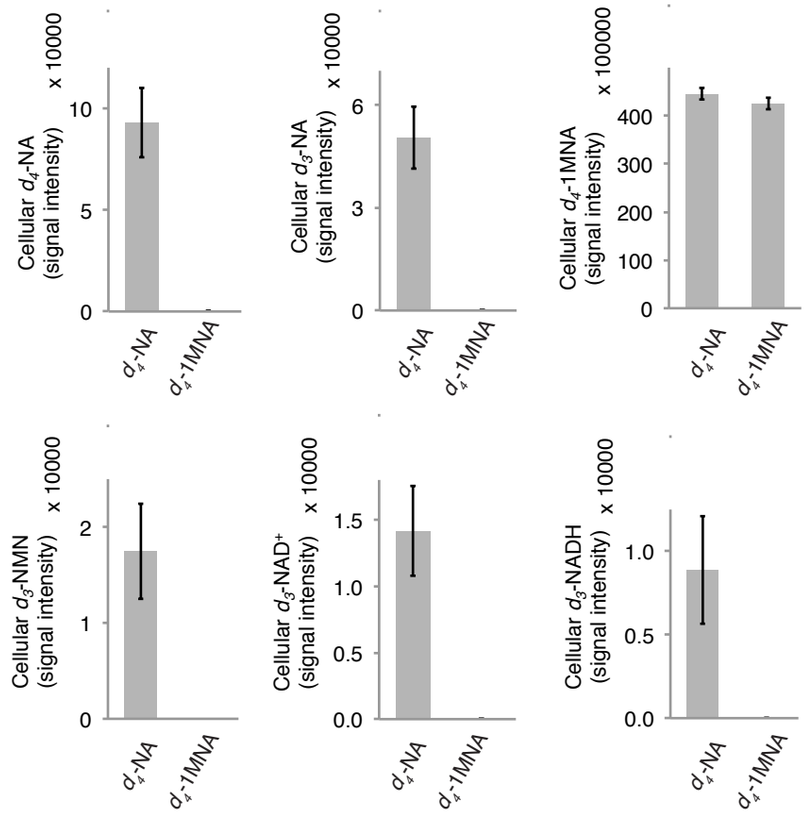

Supplementary Figure 10

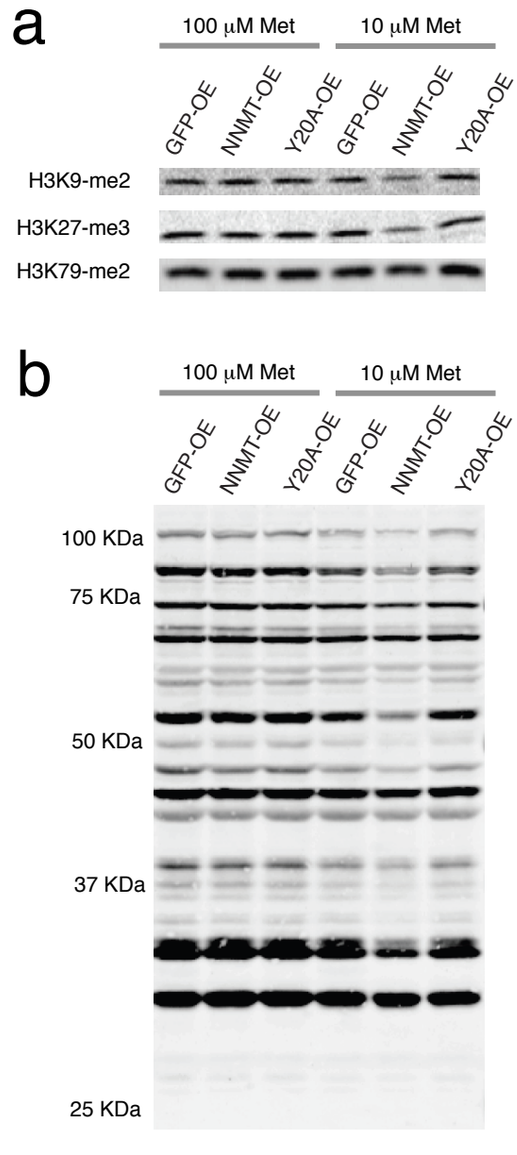

Supplementary Figure 11

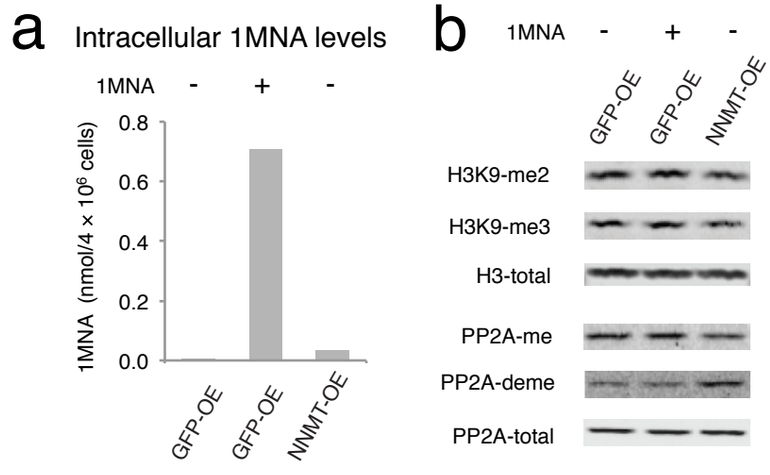

Supplementary Figure 12

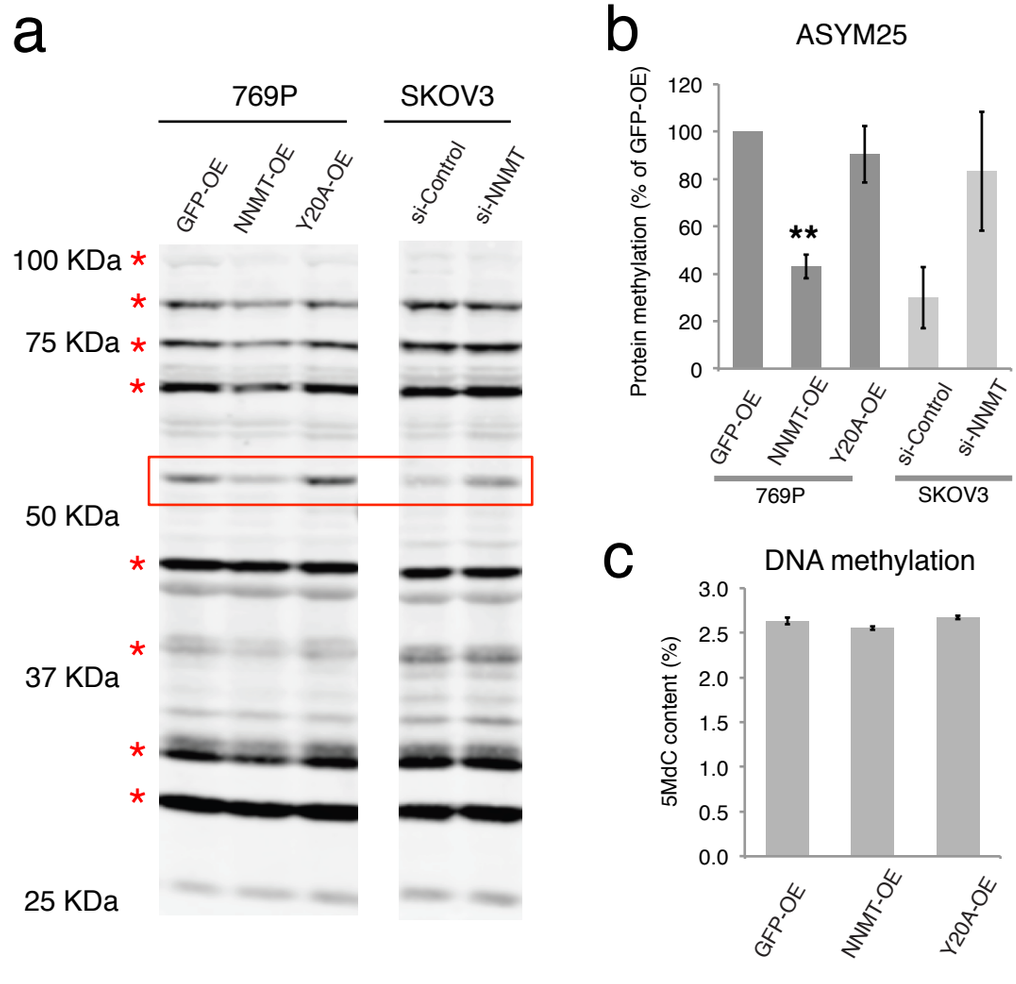

Supplementary Figure 13

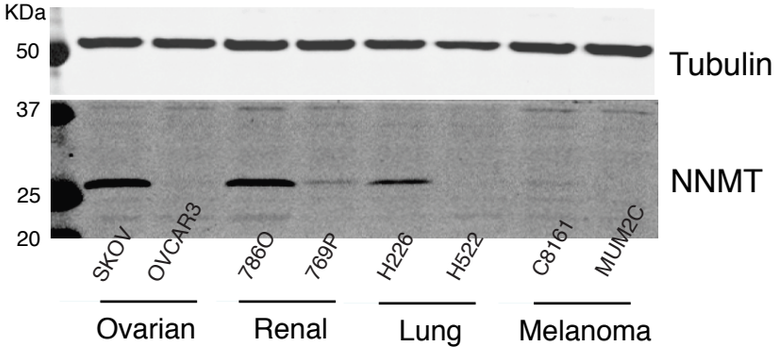

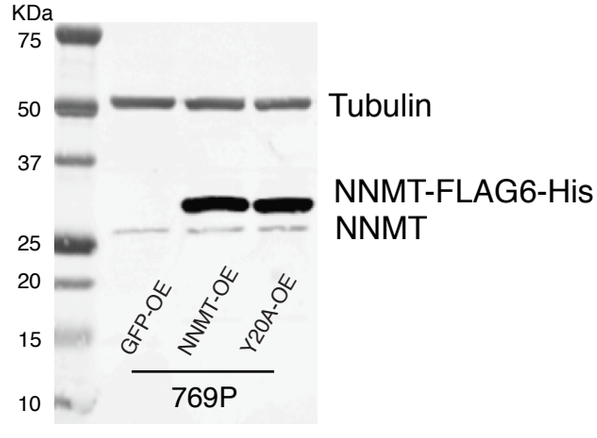

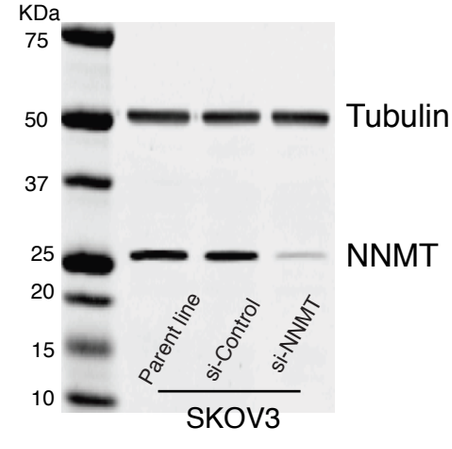

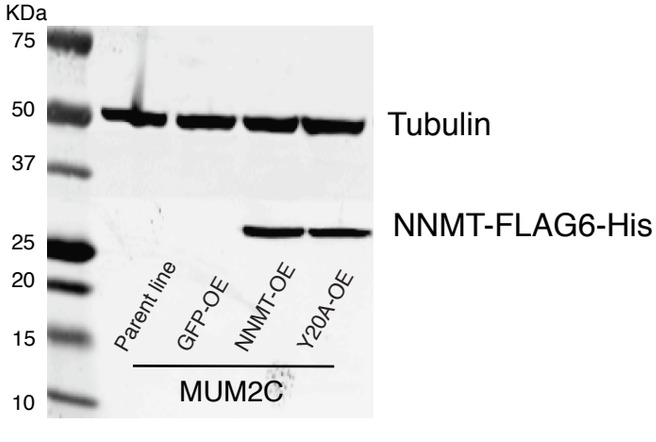

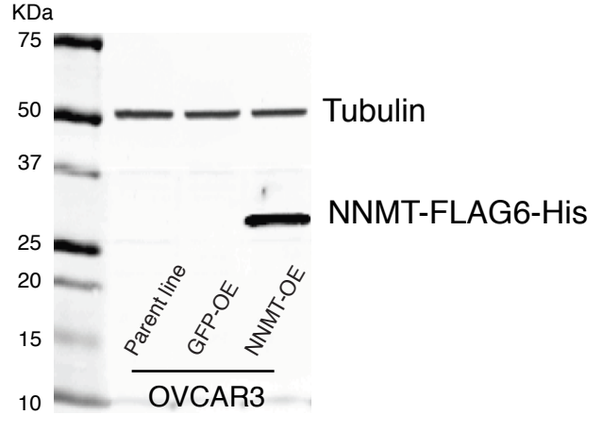

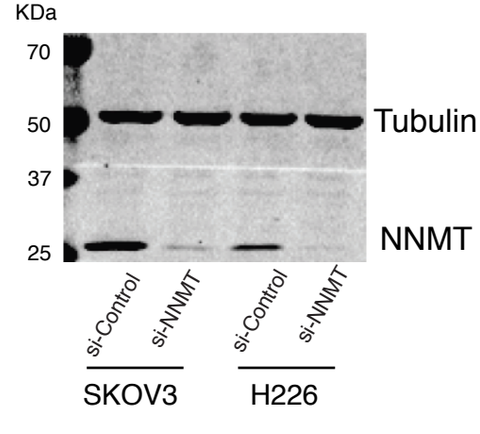

Supplementary Figure 14

a

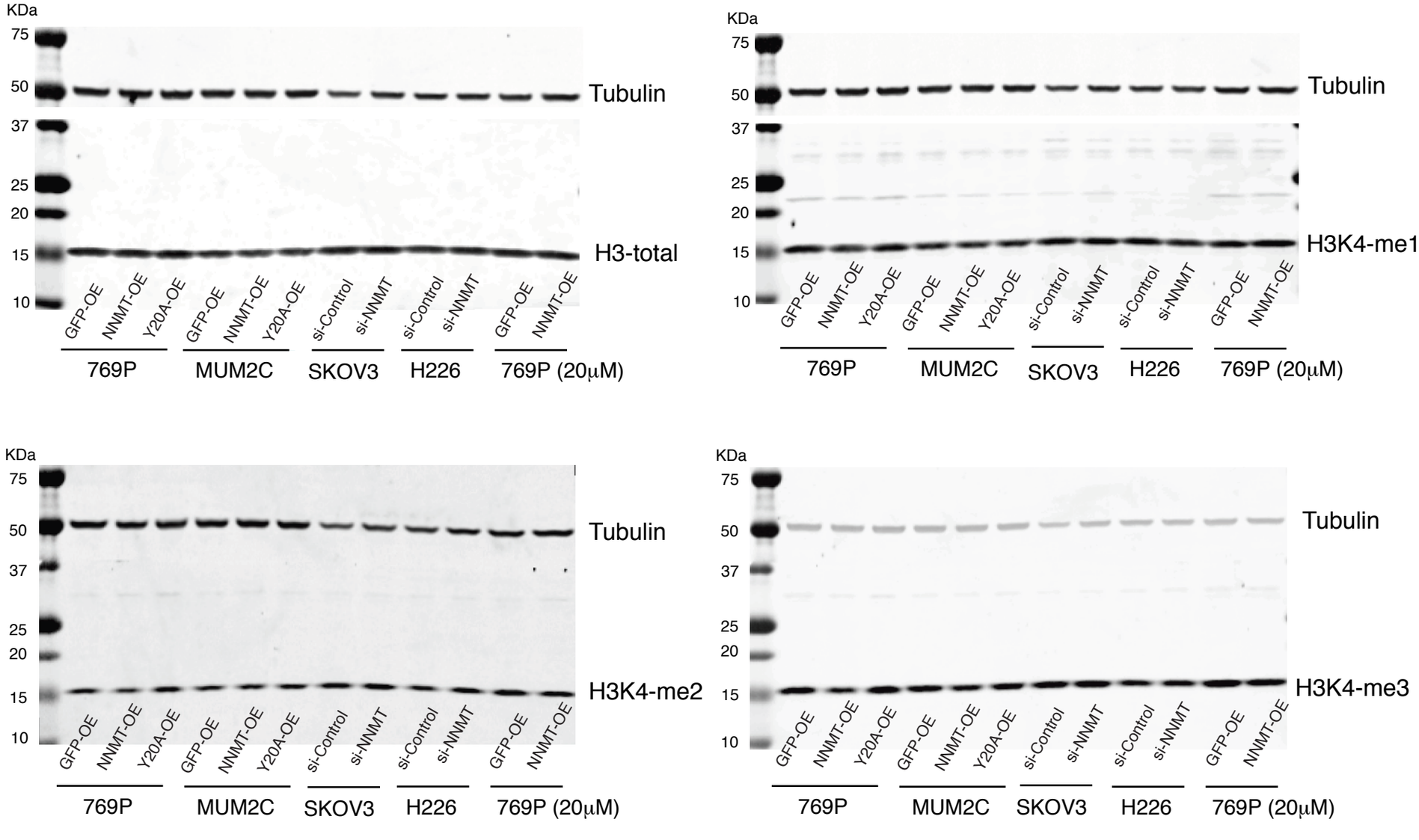

Supplementary Figure 14

b

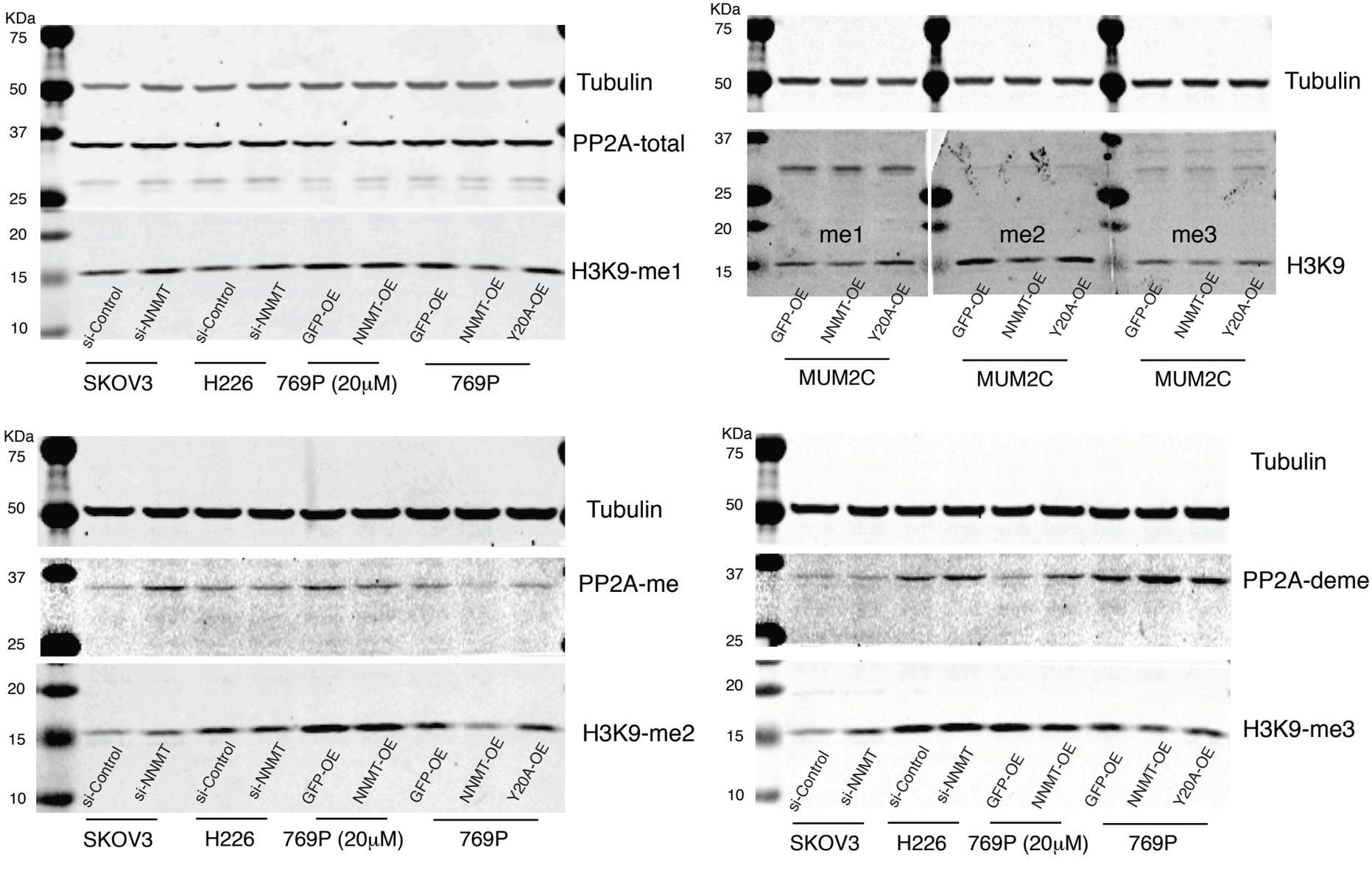

Supplementary Figure 14

c

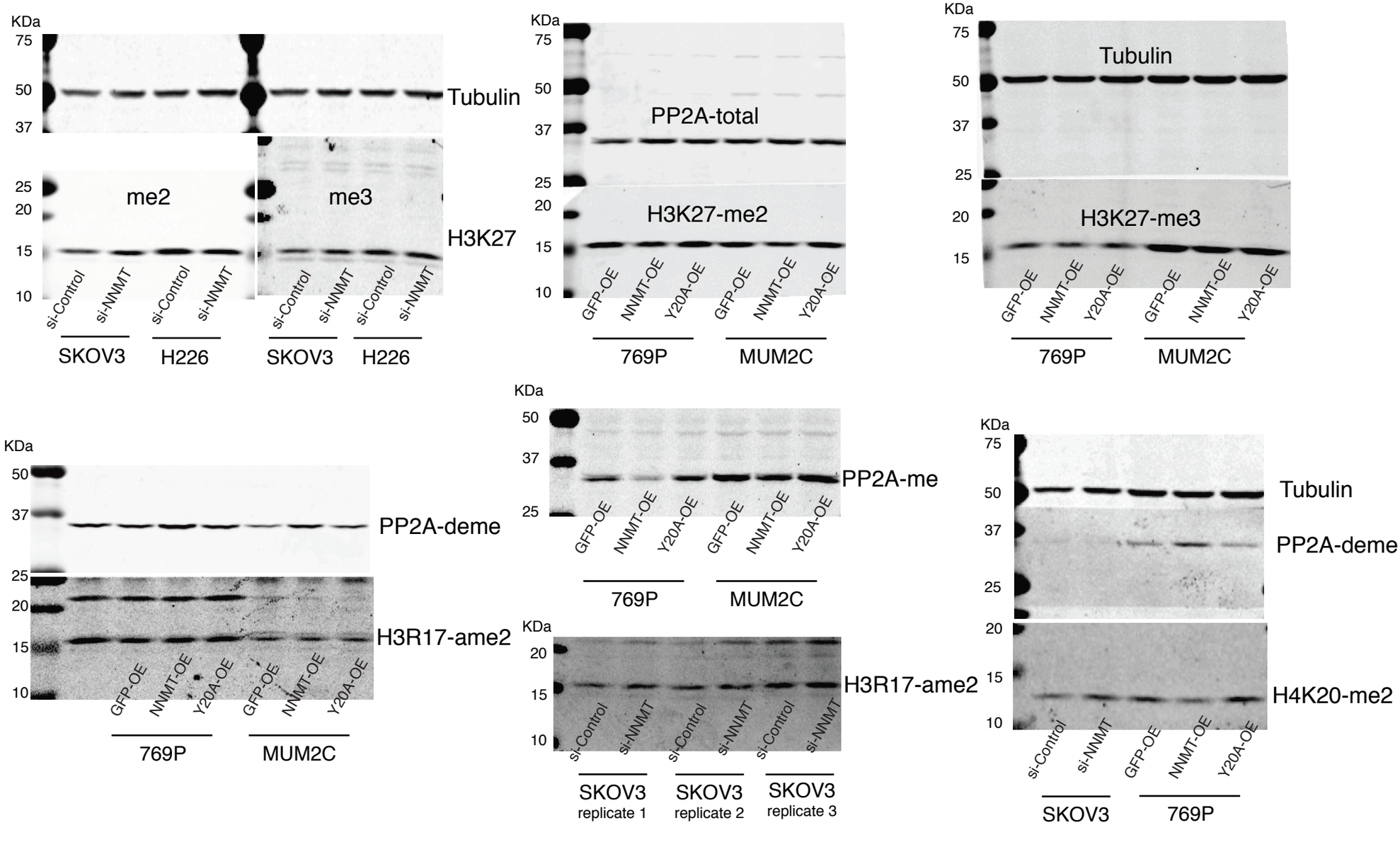

Supplementary Figure 15